Controlling Bragg gaps induced by electric boundary conditions in phononic piezoelectric plates

Nesrine Kherraz, Lionel Haumesser, Franck Levassort, P. Benard, B. Morvan

AIP | Applied Physics Letters

Controlling Bragg gaps induced by electric boundary conditions in phononic piezoelectric plates

N. Kherraz, L. Haumesser, F. Levassort, P. Benard, and B. Morvan

Citation: Applied Physics Letters **108**, 093503 (2016); doi: 10.1063/1.4943138
View online: http://dx.doi.org/10.1063/1.4943138
View Table of Contents: http://scitation.aip.org/content/aip/journal/apl/108/9?ver=pdfcov
Published by the AIP Publishing

Controlling Bragg gaps induced by electric boundary conditions in phononic piezoelectric plates

N. Kherraz,[1,2] L. Haumesser,[2] F. Levassort,[2] P. Benard,[1] and B. Morvan[1]
[1]*University of Le Havre, Laboratoire Ondes et Milieux Complexes, UMR CNRS 6294, 75 Rue Bellot, 76600 Le Havre, France*
[2]*University François-Rabelais of Tours, GREMAN, UMR CNRS 7347, 03 Rue de la Chocolaterie 41000 Blois, France*

(Received 4 December 2015; accepted 20 February 2016; published online 4 March 2016)

A Phononic Crystal (PC), constituted of a homogeneous piezoelectric plate covered by a 1D periodic arrangement of thin metallic electrodes on both surfaces, is studied. The application of Electric Boundary Conditions (EBCs) on the electrodes enables the propagation control of the ultrasonic guided waves in the PC. The band structure is investigated for different EBCs: the electrodes are either at a floating potential or they are alternately short-circuited and at a floating potential. In the latter case, a Bragg gap appears for the fundamental S_0 guided Lamb mode. These results are verified experimentally and compared to finite element calculations. A physical interpretation is also given, relying on the symmetry of the electric potential fields associated with these guided modes. © *2016 AIP Publishing LLC*. [http://dx.doi.org/10.1063/1.4943138]

Phononic crystals (PCs) generate an increasing interest in the scientific community due to their ability to control the propagation of sonic or ultrasonic waves. One of their most important properties consists of prohibiting the propagation of the elastic waves in some frequency ranges known as band gaps. Two main mechanisms are responsible for the gap formation: the periodic structuring of the different elastic materials composing the PC (Bragg gaps) and the presence of resonances localized within the inclusions (hybridization or resonance-induced gaps). In the particular case of a periodically structured waveguide, coupling may occur between guided waves. This mode coupling manifests itself in dispersion curves by veering effect and leads to the opening of gap within the first Brillouin zone.[1,2] The frequency position of these gaps depends on the lattice period of the structure, the inclusion size, and the materials' elastic properties, all of them usually fixed during fabrication of the sample. Thus, tunability of these frequencies, without destructive restructuration of the PC, will facilitate the control of the PC-based devices and remains a challenge. Up to now, PCs with a tunable frequency behavior have been proposed through several methods. For instance, mechanical action has been used to control the frequency position of the first Bragg gap by rotating the square solid inclusions in a fluid matrix PC[3] or to modulate the frequency band structure upon mechanical deformation of the elastomeric PC-matrix.[4] Active materials can also be used. Jim *et al*. have used a two-dimensional ferroelectric/epoxy composite structure; a shift in the band structure has been achieved by changing the temperature during the phase transition of the ferroelectric material.[5] However, tuning PCs properties via an external temperature field or mechanical strain implies difficulties for practical implementation. Alternatively, PCs composed by piezoelectric or piezomagnetic materials have been suggested, whose control can be easily achieved through external electric or magnetic fields.[6] In particular, it is possible to act on the band structure by varying the electric boundary conditions (EBCs);[7–9] widening and shift of the first Bragg gap has been recently realized by connecting electric capacitances to the electrodes of a piezoelectric rod stack.[10] It is worth remembering that guided waves are extensively used in electronic components, particularly in surface acoustic wave (SAW) devices such as resonators or filters that are parts of many wireless radiofrequency communication systems. Adding tunability to such devices could obviously improve the available systems and will certainly lead to new features. Several types of PCs mounted on the piezoelectric substrates involving surface acoustic waves have been proposed, the simplest configuration consisting of periodic cylindrical hole arrays that exhibit band gaps.[11,12] Moreover, pillar-based phononic crystals can produce tunable resonance-induced gaps by modifying the size and/or the materials of the pillars.[13] Casadei *et al*. used a periodic array of piezoelectric patches stuck on an aluminum plate.[14] Each patch is shunted with an inductive circuit, leading to a resonance-induced band-gap opening for the flexural waves propagating in the plate. Here, we propose a tunable piezoelectric phononic structure simply created by EBCs periodically applied along the surface of a homogeneous piezoelectric plate. Theoretical studies have already shown that Lamb waves propagating in a piezoelectric plate are sensitive to EBCs.[15,16] More recently, Zou *et al*. have studied numerically a one-dimensional PC made of alternating piezoelectric and epoxy finite plates; this structure exhibits mechanisms of mode conversion for the symmetric (S) and antisymmetric (A) Lamb waves, induced only by switching on the EBCs.[17] Our work reports an experimental demonstration of a Bragg-gap opening, arising from the setting of periodic EBCs along a piezoelectric plate which is otherwise homogeneous; the whole inhomogeneity is induced here through the externally controlled periodic EBCs.

A Pz26 piezoelectric plate[18] polarized across the thickness and covered by silver screen-painted electrodes is considered. The plate length is 58 mm, the width equals 33 mm, and its thickness is 2 mm. In order to apply periodic electric

boundary conditions, each one of the silvered areas is divided into 29 smaller rectangular electrodes of a width of 1.7 mm. The spacing between two neighboring electrodes is 0.3 mm. Particular attention is paid to deliver face-to-face electrodes on each side of the plate during the machining (see Fig. 1(a)). On each rectangular electrode, a welded wire is used to apply different EBCs. The different EBC configurations considered in this paper are given in Figure 1. In the first case (Fig. 1(b)), all electrodes are in open circuit and have a floating potential (FP) (configuration 1). In the second case (Fig. 1(c)), one in two electrodes is short-circuited with the electrode located on the other side of the plate and connected to the ground (configuration 2). Thus, the elementary cell of the resulting PC with a spatial period of $\Lambda = 4$ mm is composed of two neighboring couples of electrodes, one couple being short-circuited and grounded, while the other electrodes have a floating potential. Finally, configuration 3 (see Fig. 1(d)) corresponds to a particular case of

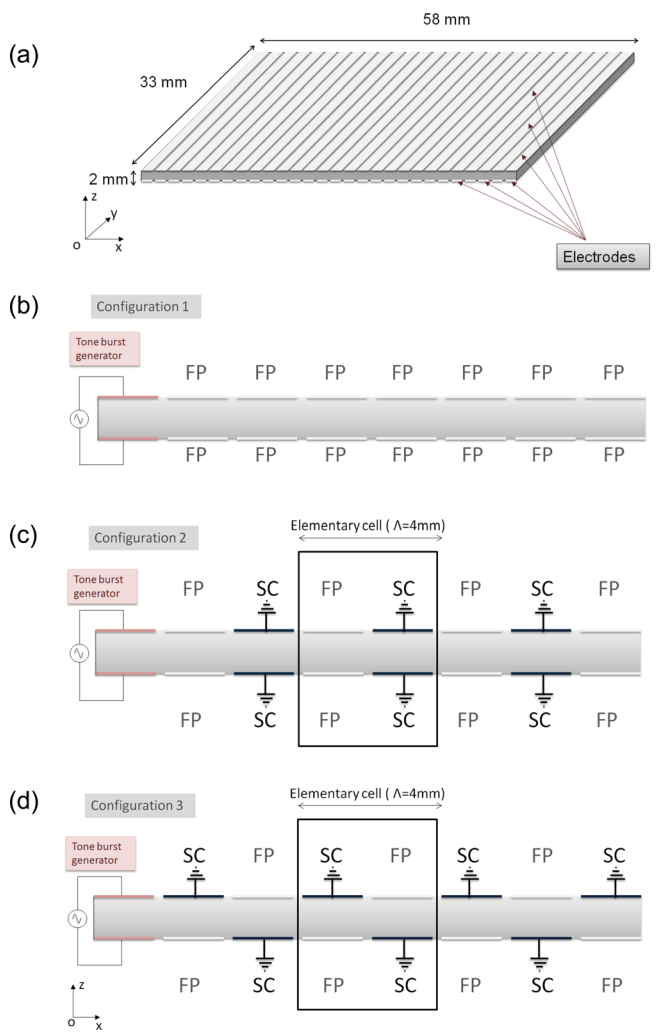

FIG. 1. Schematic representation of the piezoelectric PC together with the several EBCs applied on it. (a) Piezoelectric plate with a set of periodic electrode segments on both faces (0.3 mm separate two adjacent electrodes); the couple of electrodes at the edge of the plate is used for the Lamb wave generation. (b) Configuration 1: all electrodes have a floating potential (FP). (c) Configuration 2: the electrodes are alternatively at FP or in short circuit and connected to the ground (SC). (d) Configuration 3: antisymmetric electric boundary conditions with the short-circuited electrodes being offset with respect to each other.

antisymmetric EBCs with respect to the median plane of the plate and will be further investigated at the end of this paper. The size of the unit cell is again $\Lambda = 4$ mm, but the short-circuited electrodes are no longer facing each other and are now offset. In order to generate Lamb waves in the piezoelectric plate, a 10 V electrical tone burst (5 periods) is applied to the first couple of electrode segments located at the edge of the plate (see Fig. 1). The frequency of the signal used for the wave excitation is set to 400 kHz. Due to the symmetric excitation, we expect to generate mainly symmetric Lamb waves. A laser vibrometer is used to measure the normal component of the velocity at the surface of the plate. The sensitivity of the vibrometer is set to 50 mm/s/V. A 1D scan along the x-direction is done with a spatial step of 0.1 mm and at each position, the obtained signal is averaged 512 times to improve the signal-to-noise ratio. The corresponding spatio-temporal acquisitions are then processed. At a first stage, the signal is windowed. Only the signals measured between $x = 4.4$ mm and $x = 45$ mm are considered and a temporal signal truncation at 31 μs is used to exclude the signal corresponding to the reflected waves arising from the end of the plate. At a second stage, temporal and spatial Fourier transforms are successively applied on the data. The resulting images for the EBCs configurations 1 and 2 are shown in Fig. 2. A numerical study of the PC is developed using a finite element software (*COMSOL Multiphysics*®). Bloch-Floquet conditions are applied on the elementary cell for the two first EBC configurations and a modal analysis is performed. Dispersion curves are then obtained in the first Brillouin zone and superimposed to the experimental results in Fig. 2. In Fig. 2(a), corresponding to the case of electrodes at floating potential (configuration 1), one observes a spot between 346 kHz and 470 kHz, associated with the symmetric fundamental mode S_0. The frequency bandwidth of this mode is related to the finite number of periods of the harmonic excitation. Several supplementary spots with lower amplitudes can be also observed in the vicinity of the S_0 mode, resulting from the spatial windowing of the acquired signal. The most prominent feature of the dispersion plot of configuration 2 (Fig. 2(b)) is a strong attenuation of the S_0 incident wave, observed at the edge of the Brillouin zone (i.e., $k = \frac{\pi}{\Lambda}$) around the frequency 400 kHz. This agrees well with the band structure obtained numerically, indicating that a forbidden frequency band opens up at this frequency range. This Bragg gap opening is accompanied by a weak reflection of the incident S_0 wave observable at the same frequency but for negative wavenumbers (Fig. 2(b)).

To describe the experimentally observed attenuation for the S_0 mode, we use an experimental equivalent attenuation coefficient α, plotted in Fig. 3. This coefficient is deduced from the ratio of the amplitudes of the S_0 wave in the 2D Fourier space for the two electric boundary conditions

$$\alpha(f) = 20 \log\left(\frac{A_{FP}^{S_0}(f)}{A_{SC}^{S_0}(f)}\right), \tag{1}$$

with $A_{FP}^{S_0}$ and $A_{SC}^{S_0}$ being the amplitudes of the S_0 wave for the electric configurations 1 and 2, respectively. The attenuation

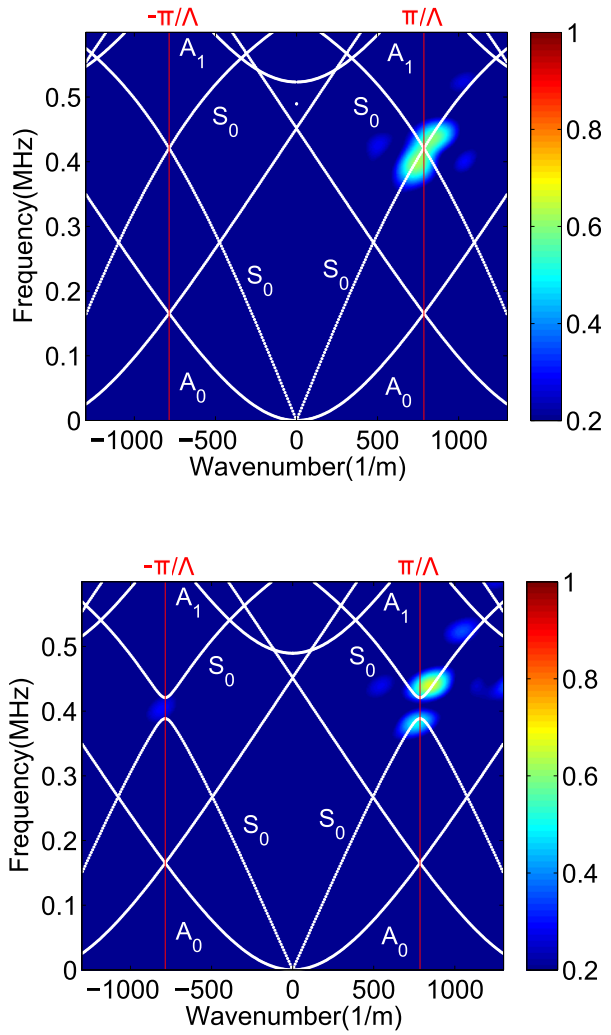

FIG. 2. Fourier transform modulus of the measured spatio-temporal signals for (a) configuration 1 and (b) configuration 2. The color map represents the amplitudes (arbitrary units); the theoretical dispersion curves are also presented for comparison (white lines).

coefficient α is not defined from an energy transmission through a finite length PC, but rather provides information on the relative attenuation of the S_0 wave during propagation. The maximum value of the attenuation, around 10 dB, is reached at the frequency 408 kHz which is in a good accordance with the location of the computed numerical band gap with center frequency 405 kHz. The weak discrepancy observed can be explained by the fact that the band structure is computed for an infinite PC, whereas measurements are performed on a finite length structure corresponding to approximately 10 periods within the PC. Concerning the antisymmetric waves A_0, it is worth noting that no forbidden frequency band is observed in the experimentally obtained dispersion plot (in agreement with the numerical predictions), when changing the electrical boundary conditions (Fig. 2(b)). In the following, in light of the electric potential fields associated with the fundamental S_0 and A_0 modes at the edges of the Brillouin zone, the opening of the band gap is discussed.

Figures 4 and 5 give the calculated electric potential fields associated with the fundamental A_0 and S_0 Lamb waves, respectively, for the two electric boundary configurations at

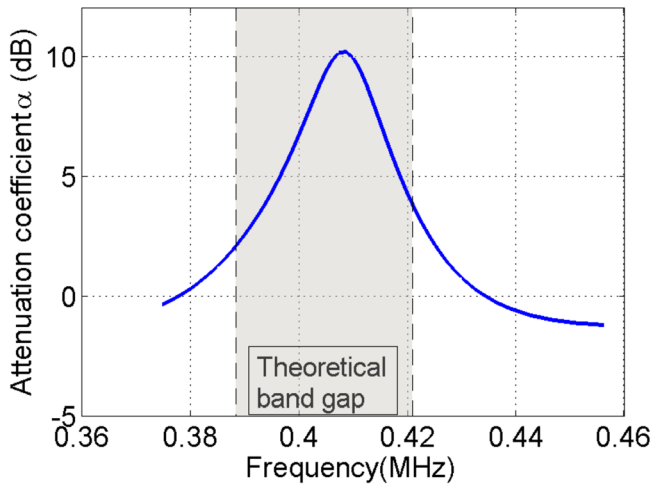

FIG. 3. Experimental attenuation coefficient as a function of frequency. The numerically computed band gap is shown in the gray-shaded region, delimited by the two dashed lines.

the particular wavelength $\lambda_{S_0} = \lambda_{A_0} = 2\Lambda$ corresponding to the edge of the first Brillouin zone. We remember that the flexural A_0 Lamb wave, which is an antisymmetric wave, keeps unchanged the thickness of the plate at any x position. Consequently, we expect that the electric potential difference between electrodes on both sides of the piezoelectric plate remains null and short-circuiting these electrodes should not affect the propagation of the wave. Indeed, this is confirmed by the results illustrated in Figs. 4(a) and 4(b), where no significant difference is observed between the electric potential associated to the A_0 wave for both electric boundary configurations considered up to here.

Inversely, the symmetric mode S_0, which corresponds to a compressional wave, implies variations of the thickness (see Fig. 5). The piezoelectric plate is polarized across its thickness so that the electro-mechanical coupling is maximum for elastic strains along z-direction. Thus, opposite potentials appear on both sides of the plate during the propagation of the fundamental S_0 waves. Figure 5 clearly

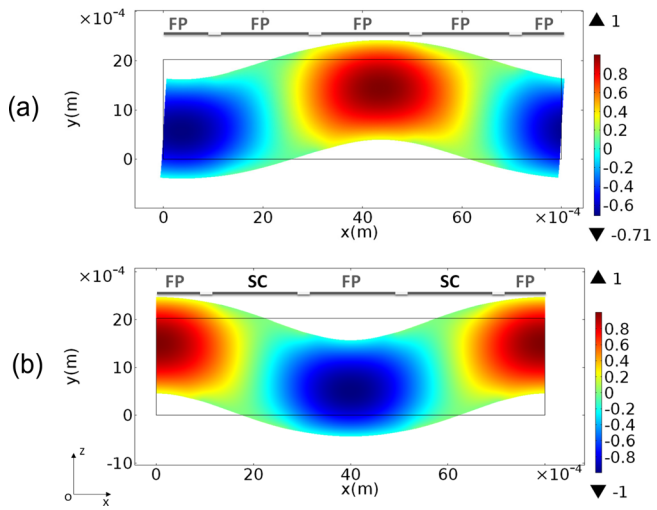

FIG. 4. Calculated color map of the electric potential and mode deformation shape associated to A_0 wave at $f = 165$ kHz for an infinite Pz26 plate in the xz-plane for: (a) electric boundary configuration 1, and (b) electric boundary configuration 2.

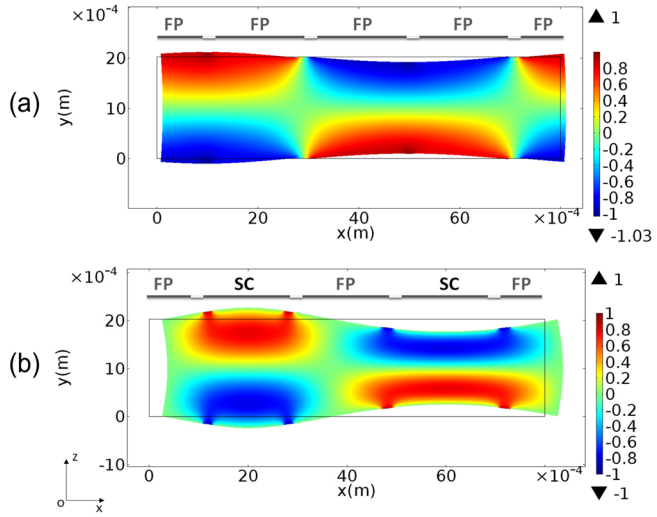

FIG. 5. Calculated color map of the electric potential and mode deformation shape associated to S_0 wave for an infinite Pz26 plate in the xz-plane for: (a) Frequency $f = 420$ kHz and electric boundary configuration 1 and (b) frequency $f = 388$ kHz and electric boundary configuration 2.

illustrates the effects related to the short circuit (SC) of a couple of electrodes. In the first configuration case (Fig. 5(a)), the small distance (kerf = 0.3 mm) between two adjacent electrodes does not create a significant discontinuity of the electric potential for the S_0 Lamb wave with a wavelength of $\lambda = 8$ mm. The wave propagates as the plate was covered with uniform electrodes. On the contrary, an electric pattern is created along the wavelength λ since one couple of electrodes is short-circuited and connected to the ground (Fig. 5(b)). Thus, the periodic EBCs applied on the electrodes enable local variations of the effective elastic properties of the piezoelectric plate, and depending on their polarization, propagation of Lamb waves can be affected by this electric control. The band structure of the device under study can be easily tuned by changing the EBCs, as confirmed by the numerically computed dispersion plots shown in Fig. 6. Indeed, the Bragg gap associated with the S_0 wave can be shifted towards the low-frequency range by simply changing the width Λ of the elementary cell. For instance, a gap can be opened up at about 208 kHz (see Fig. 6(a)) by doubling the number of consecutive short-circuited electrodes and

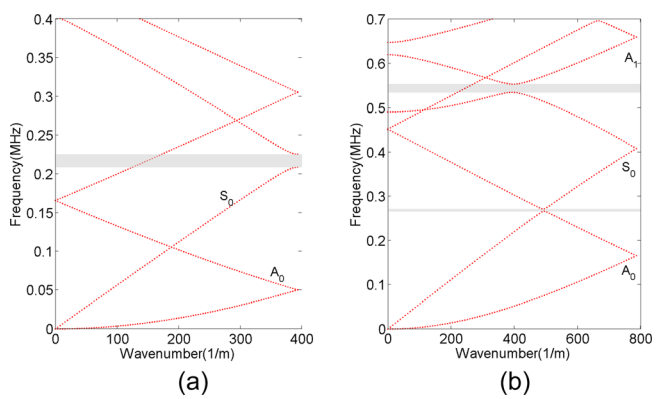

FIG. 6. Calculated band structure for (a) the symmetric EBC configuration whose elementary cell of length $\Lambda = 8$ mm (two FP succeeded by two SC electrodes) and (b) an antisymmetric EBC (configuration 3). The gray-shaded rectangles represent the band gaps regions.

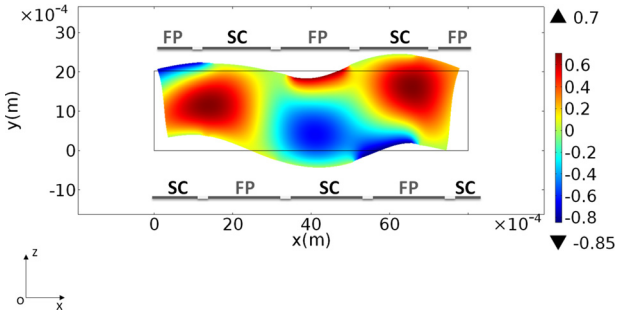

FIG. 7. Calculated color map of the electric potential and mode deformation shape at $f = 265$ kHz for an infinite Pz26 plate in the xz-plane for the electric boundary configuration 3.

electrodes at floating potential, entailing an increase in the lattice parameter of the periodic structure ($\Lambda = 8$ mm).

Furthermore, a coupling between Lamb modes of different symmetries can be observed when applying antisymmetric EBCs (see Fig. 1(d)). Figure 6(b) gives the band structure of the PC for such EBCs. Here, all the Bragg gaps at the edge of the Brillouin zone are closed, whereas some gaps within the first Brillouin zone, involving waves of different symmetries, are opened. This property was previously stated in PCs made of plates with periodic surface grating.[19] For the considered EBCs, a coupling between S_0 and A_0 modes leads to an anti-crossing of the dispersion curves and the opening of a gap around 265 kHz. The corresponding electric potential field distribution is plotted in Fig. 7 at the particular frequency $f = 265$ kHz. The resulting image is a hybrid pattern mixing a compressional and a flexural mode. One can also notice a coupling between S_0 and A_1 modes at 533 kHz. The reconfigurable and simply tunable PC presented in this paper offers a great ease of use due to the electric nature of the control. Some basic controlled switches connected between electrodes allow the opening of gaps in the band structure of the PC. The use of Lamb waves with various dispersion properties and symmetries offer a large number of possibilities for band structure engineering. Moreover, this device can be easily implemented in integrated electronic circuits and could be efficiently used for the realization of tunable frequency filters or resonators.

We gratefully acknowledge the help of Claire Bantignies (VERMON SA, Tours, FRANCE) for sample preparation. This work was supported by the French National Research Agency in the framework of the project MIRAGES ANR-12-BS09-0015 and by the Acoustic Federation of the North-West (FANO FR CNRS 3110).

[1]A. E. Bergamini, M. Zündel, E. A. F. Parra, T. Delpero, M. Ruzzene, and P. Ermanni, J. Appl. Phys. **118**, 154310 (2015).
[2]B. R. Mace and E. Manconi, J. Acoust. Soc. Am. **131**, 1015 (2012).
[3]C. Goffaux and J. Vigneron, Phys. Rev. B **64**, 075118 (2001).
[4]K. Bertoldi and M. Boyce, Phys. Rev. B **77**, 052105 (2008).
[5]K. Jim, C. Leung, S. Lau, S. Choy, and H. Chan, Appl. Phys. Lett. **94**, 193501 (2009).
[6]J.-F. Robillard, O. B. Matar, J. Vasseur, P. Deymier, M. Stippinger, A.-C. Hladky-Hennion, Y. Pennec, and B. Djafari-Rouhani, Appl. Phys. Lett. **95**, 124104 (2009).
[7]A. Kutsenko, A. Shuvalov, O. Poncelet, and A. Darinskii, J. Acoust. Soc. Am. **137**, 606 (2015).

[8]A. Bergamini, T. Delpero, L. D. Simoni, L. D. Lillo, M. Ruzzene, and P. Ermanni, Adv. Mater. **26**, 1343 (2014).
[9]B.-I. Popa, D. Shinde, A. Konneker, and S. A. Cummer, Phys. Rev. B **91**, 220303 (2015).
[10]S. Degraeve, C. Granger, B. Dubus, J.-O. Vasseur, M. P. Thi, and A.-C. Hladky-Hennion, J. Appl. Phys. **115**, 194508 (2014).
[11]S. Benchabane, A. Khelif, J.-Y. Rauch, L. Robert, and V. Laude, Phys. Rev. E **73**, 065601 (2006).
[12]B. Bonello, C. Charles, and F. Ganot, Appl. Phys. Lett. **90**, 021909 (2007).
[13]M. Oudich, Y. Li, B. M. Assouar, and Z. Hou, New J. Phys. **12**, 083049 (2010).
[14]F. Casadei, T. Delpero, A. Bergamini, P. Ermanni, and M. Ruzzene, J. Appl. Phys. **112**, 064902 (2012).
[15]H. F. Tiersten, J. Acoust. Soc. Am. **35**, 234 (1963).
[16]M. Y. Dvoesherstov, V. Cherednik, and A. Chirimanov, Acoust. Phys. **50**, 512 (2004).
[17]X.-Y. Zou, B. Liang, Y. Yuan, X.-F. Zhu, and J.-C. Cheng, J. Appl. Phys. **114**, 164504 (2013).
[18]See http://www.ferroperm-piezo.com for the properties of the piezoelectric materials.
[19]M. Bavencoffe, A.-C. Hladky-Hennion, B. Morvan, and J.-L. Izbicki, IEEE Trans. Ultrason. Ferroelectr. Freq. Control **56**, 1960 (2009).